REINFORCEMENT AGAINST CRACK PROPAGATION OF PWR ABSORBERS BY DEVELOPMENT OF BORON-CARBON–HAFNIUM COMPOSITES

B. PROVOT, P. HERTER
Laboratoire d'Etudes des Matériaux Absorbants,
CEA,
Saclay, Gif-sur-Yvette,
France

XA0053635

Abstract

In order to improve the mechanical behaviour of materials used as neutron absorbers in nuclear reactors, we have developed CERCER or CERMET composites with boron and hafnium. Thus a new composite B_4C/HfB_2 has been especially studied. We have identified three kinds of degradation under irradiation (thermal gradient, swelling due to fission products and accidental corrosion) that induce imposed deformations cracking phenomena. Mechanical behaviour and crack propagation resistance have been studied by ball-on-three-balls and double torsion tests. A special device was developed to enable crack propagation and associated stress intensity factor measurements. Effects of structure and of a second phase are underline. First results show that these materials present crack initiation and propagation resistance much higher than pure boron carbide or hafnium diboride. We observe R-Curves effects, crack bridging or branching, crack arrests, and toughness increases that we can relate respectively to the composite structures.

1. INTRODUCTION: DAMAGES IN NEUTRON ABSORBERS DURING IRRADIATION

Neutron absorbers in nuclear control rods consist in boron compounds in metallic cladding. The neutron capture by boron atoms leads to the creation of helium atoms which cause an important swelling of the materials (~0,15 vol. % per 10^{20} captures.cm^{-3} corresponding to 80 cm^3 He/cm^{-3} B_4C) [1] according to the reaction:

$$^{10}B + n \rightarrow {}^4He + {}^7Li + 2{,}6\ MeV.$$

This reaction causes material damage due to atom recoil, swelling and thermal stresses. In pressurized water reactors (PWRs), a high flux depression involves a differential irradiation induced swelling along the pellets radius and thus induces high stresses at the pellet's periphery, but no thermal stresses. Associated with neutron damage, this leads to fragmentation starting from the surface of the material.

In Fast Breeder Reactors (FBRs), contrary to PWRs, neutrons penetrate the bulk of the pellets. This leads to an homogeneous volume heat release, a temperature gradient of about 1000°C between pellet's centre and surface and tangential stresses, which largely overcome material's strength, causing premature rupture of the absorbers (radial cracks). Associated with bulk neutron damage, this leads to a complete fragmentation [2].

In both type of reactors, absorber fragments may segregate by gravity to the bottom of the rods or stick between pellet and clad. Associated with irradiation induced He swelling, this can induce a significant damage to the absorber's cladding. In PWRs, if a seal loss of the clad occurs, pellets may be corroded by the primary coolant. Corrosion pits induce then crack initiations leading to premature failure [3].

All these absorber phenomena involve imposed deformation cracking mechanisms: thermal dilatation (FBR), oxide phase dilatation (PWR corrosion) and irradiation induced swelling (creation of helium in PWR and FBR pellets) (see Figure 1).

This work displays the mechanical study of several composites based on boron carbide or hafnium diboride matrixes. The purpose is to characterize the materials (strength, rupture modes and crack propagation resistance) and to identify reinforcement modes towards cracking in comparison with associated single phase materials.

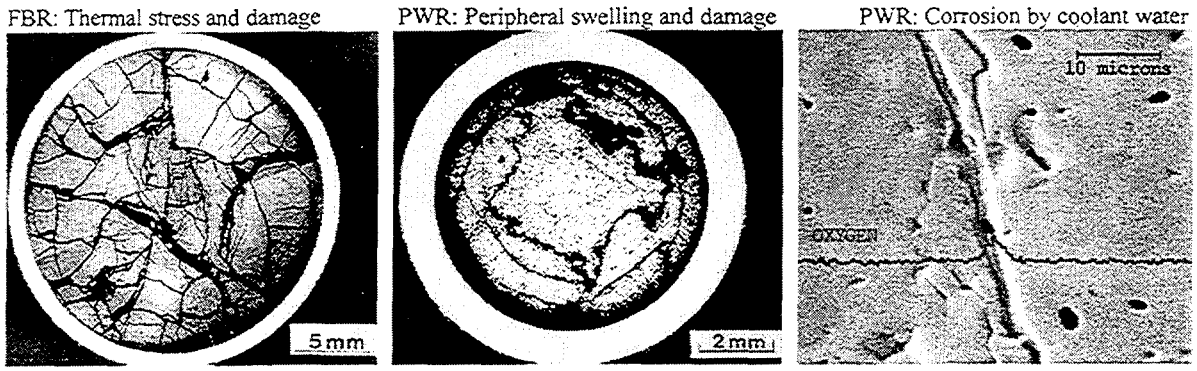

FIG. 1. Damage modes of pellets during irradiation

2. DEVELOPMENT OF MATERIALS

The aim is to give to our materials sufficient reinforcement to stop or minimize crack propagation and to enable them to conserve a sufficient cohesion though a high mechanical damage. The reinforcement of a ceramic can take different routes. Most frequently, a second phase is introduced (metal or ceramic) and different mechanisms are taken into account [4]. In a cermet, the metallic component (continuous or dispersed in a matrix) confers globally some ductility. In the case of a reinforcement by ceramic inclusions, we try to create a network in which cracks will propagate with difficulty. A process zone can develop in the vicinity of the crack tip leading to a significant decrease of the crack driving force. The more frequent mechanisms acting in a process zone are residual stresses due to differential thermal expansion coefficient or phase transformation, or micro-cracking due to differential elastic constants.

Several composite materials have been fabricated by hot uniaxial pressing of mixed ceramic and/or metallic powders. Fine micrometric HfB_2 or B_4C powders have been mixed with fine powders like metallic hafnium [4] or ceramic hafnium oxide, or particles of hafnium diboride [5, 6]or metallic hafnium. Table I shows the different studied materials. We obtained two main grades of materials: fine grained homogeneous composites named "microdispersed" and heterogeneous composites in which reinforcement is constituted by large secondary phase aggregates or inclusions named, "macrodispersed" (by adjusting the hot pressing parameters, macrodispersed materials are obtained by coalescence from microdispersed powders).

TABLE I. DIFFERENT TYPES OF MATERIALS AND COMPOSITES STUDIED

Matrix	**Symbol**	**Additive**	**Second phase after sintering**
HfB_2	A		
	A1	Hf micrometric powder	microdispersed HfB, HfB_2, HfC
	A2	HfO_2 micrometric powder	microdispersed HfO_2
B_4C	B		
	B1	micrometric HfB_2 powder	macrodispersed $HfB_{2\text{-}d}$
	B2	HfB_2 submillimetric agglomerates	HfB_2 submillimetric agglomerates macrodispersed
	B3	Hf submillimetric agglomerates	Hf submillimetric agglomerates macrodispersed

3. EXPERIMENTAL PROCEDURE

3.1 Ball-on-three-balls biaxial bending test [7, 8]]

The load is applied thanks to a central ball on the upper side of a thin disc (Figure 2). The disc is supported on its lower side periphery by three balls regularly distributed on a concentric ring. In this case, radial and tangential stresses are equal and maximal at the centre of the sample, and are expressed by an analytical simple plate theory formula of the form:

$$\sigma_{rr}^{max} = \sigma_{\theta\theta}^{max} = P \times F(\nu, geometry)$$

P being the load and ν the Poisson's ratio. An estimation of the Young modulus is also obtained from the central deflection w. Thus measurement of the critical load at the sample's collapsing enables to calculate material strength.

This test is particularly well adapted to characterization of very hard and brittle ceramic materials as boron carbide or hafnium diboride, and gives better results than 3-points or 4-points bending tests (These tests are however kept for samples with strain gauges for measurement of Poisson's ratio).

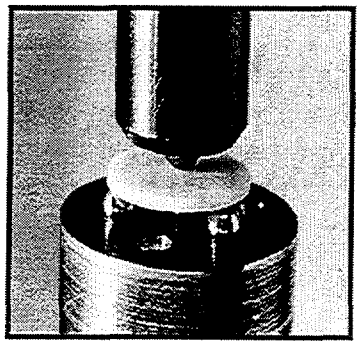

FIG. 2. Ball-on-three-balls bending test

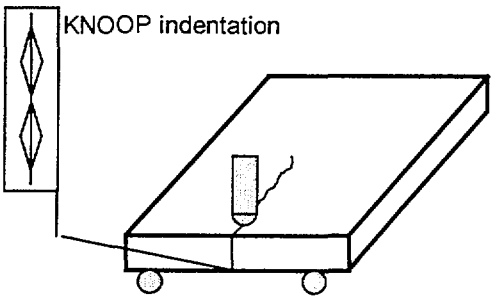

FIG. 3. Double torsion test

3.2. Double torsion test [9]

Double torsion test allows to measure ceramic toughness K_{IC}. Samples are thin rectangular plates in which a notch is prepared (Figure 3). The notch is submitted to bending and the crack propagates from the tip of the notch. The sample in supported by four balls and the load is also applied with a ball on the beginning of the notch. The stress intensity factor is proportional to the load P and depends on geometry and elastic constants. It is expressed by analytical formula:

The critical value K_{IC}, where the crack propagates, is then obtained by a formula like:

$K_{IC} = P_c \times G(elastic\_constants,\ geometry)$, where P_c is the critical load (Figure 4).

Thus we can determine the evolution of stress intensity factor as a function of crack length via the load. In the case of a brittle homogeneous material, crack propagates for a constant value of critical load (Figure 5). If crack shielding occurs (deflection, bridging, arrest), the deflection-load curve is perturbed, with (Figure 6) or without (Figure 7) global reinforcement. In this second case, material demonstrate a R-Curve effect i.e. an increasing toughness as crack propagates in the material.

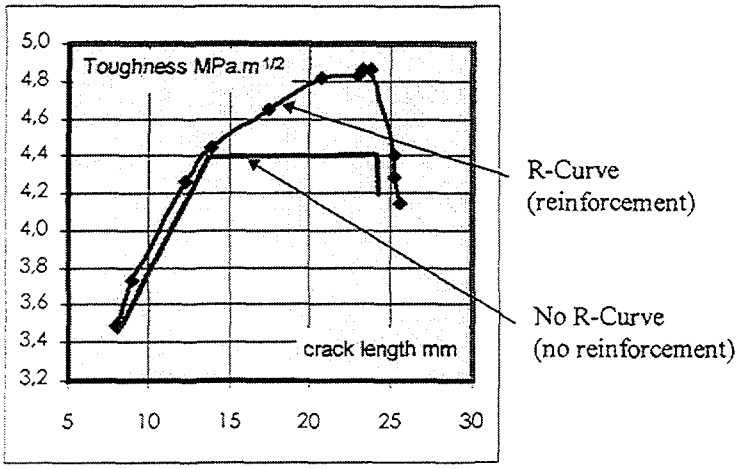

FIG. 4. R-Curve effect

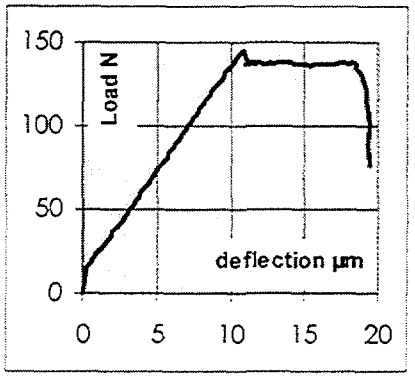

FIG. 5. Brittle homogeneous material

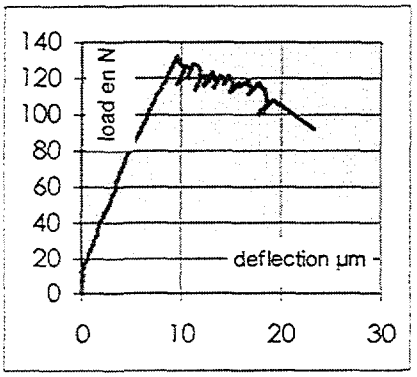

FIG. 6. Crack shielding without reinforcement

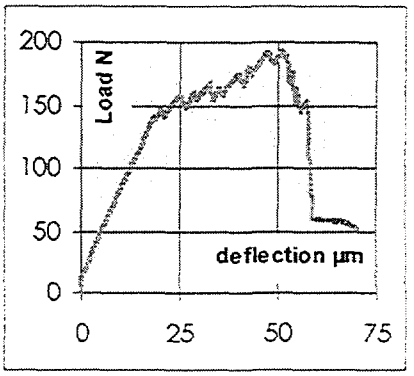

FIG. 7. Crack shielding with reinforcement

3.3 Thermal gradient crack test

This test consist in applying to a ceramic thin disc a thermal gradient by focusing with two elliptic reflectors high power halogen bulb light at the centre of the sides of the sample which is cooled at its periphery. The parabolic like temperature of the pellet's surface is measured by thermocouples and the light power is measured with a power meter.

Testing no-notched discs leads to thermal strength determination. The materials are submitted to increasing thermal gradient, so far as they crack and/or break. Measurement of thermal gradient leads to thermal gradient strength according to classical 1-D radial analytical formula.

Testing notched discs leads to thermal gradient toughness. An analytical method based on superposition principle in mechanics leads to toughness calculation via a Gauss-Chebychev resolution. Thus at crack start, toughness K_{IC} is obtained through an analytical formula depending on crack length, geometry, material's thermo-mechanical properties, and lamp power. The toughness calculations is confirmed by a finite element calculation (CASTEM 2000). Finite elements are later used for crack propagation calculation.

This test offers the possibility to proceed to a step by step propagation experiment, where the sample is removed and examined by scanning electron microscopy (SEM) at each step. Items obtained are: crack length, reinforcement mechanisms (crack arrest before, inside or after an inclusion or at an to interface inclusion-matrix), calculation of toughness at crack start and crack arrest in order to quantify reinforcement mechanism like:

$$K_{IC}^{composite} = K_{IC}^{matrix} + \Delta K^{inclusion}$$

At last, we can obtain a curve describing a global reinforcement as a function direct measurement of crack length identifying each respective reinforcement mechanisms (see Figure 8).

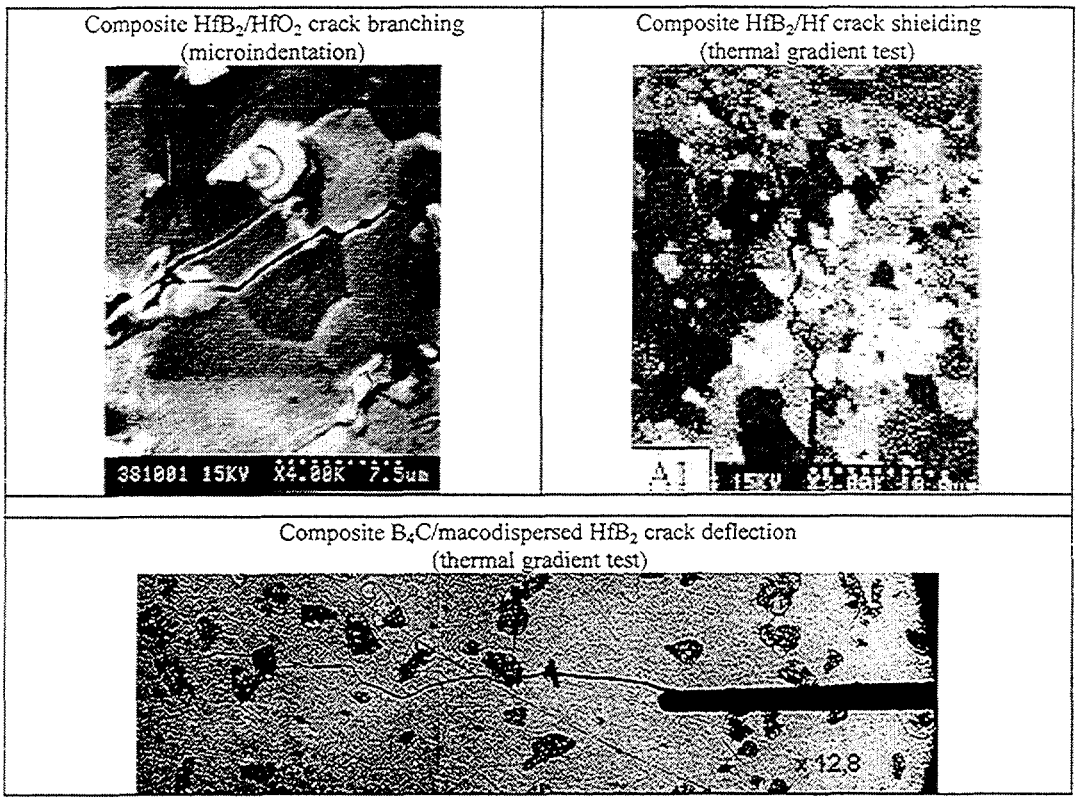

FIG. 8. Different crack morphologies obtained

4. RESULTS AND DISCUSSION

Strengths and toughness have been respectively measured by ball-on-three-balls [10] and double-torsion [11] tests. Results of these experiments are reported in Table II . The strength can be strongly affected, especially in the case of "macrodispersed" composites because of the change in critical flaw size. However, strength is not a critical material parameter versus the loading conditions during pellets irradiation. The aim is not to avoid crack initiation but to avoid fragmentation. Toughness or crack arrest are certainly more relevant parameters for the considered application.

Optical and SEM observations, on polished or fractured surfaces reported in Figure 8, allow the mechanisms of crack propagation and of crack arrest to be understood. In all composites, A1 excepted, the crack propagation is disturbed by the second phase. Deflection by the inclusions, shielding by the particles and branching of the crack can be observed. Inclusions, hafnium-rich phases, residual stressed areas and microcracked particles [12] play a role. The composite inclusions delay or sometimes stop simple intragranular brittle cracking of HfB_2 or B_4C matrix. The efficiency of these reinforcement phenomena is confirmed by the measurements of the mechanical properties. Compared with single-phased materials, the fracture toughness increases from 31 up to 62 %. An R-curve is also sometimes observed, probably because of crack bridging by particles. Only A2 composite does not present a R-curve effect because of the small size of inclusions. B2 composite exhibits moreover a dissipative behaviour during strength measurements probably due to the presence of microcracked aggregates.

In all cases, these results confirm the possibility to delay complete and premature collapse of ceramics.

TABLE II. TEST RESULTS OBTAINED BY BALL-ON-THREE-BALLS BIAXIAL BENDING, DOUBLE TORSION AND THERMAL GRADIENT TESTS

Symbol	Brittle (B) or Dissipative (D) rupture	R-Curve effect	Young modulus (MPa)	Strength (MPa)	Weibull coefficient m	K_{IC} (MPa.m$^{-1/2}$)
A	B	no	418	398	10	3,1
A1	B	yes	416	688	7	4,8
A2	B	no	405	527	16	5,1
B	B	no	310	497	7	3,6
B1	D	yes	242	264	17	5
B2	D	yes	207	176	10	5
B3	D	yes	147	120	5	

REFERENCES

[1] ZUPPIROLLI, L., et al., Phil. Mag. A, 60-5 (1989) 539-551.
[2] STOTO, T., et al., J. Appl. Phys., 68-2 (1990) 3198-3206.
[3] DESCHANELS, X., Key Eng. Mat., Vol. 13 (1996) 189-198.
[4] EVANS, A.G., J. Am. Ceram. Soc., 73-2 (1990) 187-206.
[5] GOSSET D., et al., JJAP, Series 10 (1994) 216-219.
[6] CHEMINANT, P., et al., Key Eng. Mat., Vols 132-136 (1997) pp.643-646.
[7] KIRSTEIN, A.F., J. of research of the Nat. Bur. of Stand. - C Eng. and Instrumentation, Vol. 70C, N°4, (Oct.-Dec. 1966).
[8] DE WITH, G., J. Am. Ceram. Soc., 72 [8] (1989) 1538-41.
[9] BOUSSUGE, M., PhD Thesis ENSMP, Paris, (1984).
[10] DE WITH, G., et al., J. Am. Ceram. Soc., 72-8 (1989) 1538-1541.
[11] FOURNEL, B., PhD Phesis, Ecole Nationale Supérieure des Mines de Paris, Paris, (1991).
[12] FABER, K.T., et al., Proc. Int. Conf. Fract., 4th, (1977) I 529-56.